Journal of Porous Materials
https://doi.org/10.1007/s10934-022-01264-8

Mesoporous Cellular Foam (MCF): an efficient and biocompatible nanomaterial for the controlled release of Chlorambucil

Juliana M. Juárez[1] · **Jorgelina Cussa**[1] · **Oscar A. Anunziata**[1] · **Marcos B. Gómez Costa**[1]

Accepted: 5 May 2022
© The Author(s), under exclusive licence to Springer Science+Business Media, LLC, part of Springer Nature 2022

Abstract
Nanotransporters have entered a great deal of exploration attention because of their promising openings in medicine delivery. We propose in this work, the Mesostructured siliceous cellular (MCFs) nanomaterial as a promising new host for drug delivery systems because both their specific physicochemical properties, in addition to the high biocompatibility, biodegradability, and low toxicity, make them seductive for controlled medicine release operations. Chlorambucil, is used as a chemotherapy drug administered for treating some types of cancer, chronic lymphocytic leukemia, low-grade non-Hodgkin's lymphoma, Hodgkin's lymphoma and ovarian cancer.

Chlorambucil-loaded Mesostructured cellular foam (MCF-CLB) was prepared and characterized by XRD, TEM, UV-Vis DRS, FTIR, and texture analysis determining the adsorption capacity and its release, achieving the required therapeutic efficacy.

The release of the drug was conducted by simulating the physiological conditions to reproduce the conditions of the organism. The mechanism of drug release from the MCF-CLB host was evaluated. Different mathematical models were used to adjust the experimental data, the best model describing the phenomenon under study over the entire period is the Weibull model. The auspicious results we attained for the release of the drug using the new material. The main advantage of this release is that the rate of release is fast at the beginning and then gradually decreases until 24 h practically all the drug contained in the carrier is released (>95%).

Keywords MCF · CHLORAMBUCIL · NANOTRANSPORTERS · DRUG-DELIVERING DEVICE · NANOSCALE MEDICINE

1 Introduction

Nanotransporters have received a great deal of research attention because of their promising opportunities in drug delivery [1–5]. Attempting to minimize the secondary adverse events of anticancer drugs and enhance the therapeutic rate, various nanotransporters have been devised, including dendrimers [6, 7], liposomes [8, 9], inorganic nanoparticles, and polymeric nanoparticles [10–13]. Although such methods can be useful, there are current safety considerations and concerns about the biodegradability and long-term toxicity of synthetic nanoscale target delivery carriers. In particular instance of antitumor drugs, tailoring the delivery system with selected ligands have increased anticancer effectiveness by achieving a tumor-targeted delivery system that has minimal adverse impact on healthy tissues [14]. Likewise, polymer-, lipid- and polymer and molecular inorganic nanoparticulate systems (chlorambucil loaded graphene- oxide nanocarrier), have been explored as recent progress in molecular mapping of cancer cells and targeted delivery of drugs to selected locations [15]. The amphiphilic conjugates self-assembled into nanoparticles exhibit substantially in vitro antitumor therapy against many human cancer cells [16]. New iron oxide nanoparticles attached to an anticancer drug to treat leukemia have recently been reported [17]. Chlorambucil (CLB), is a substance classified as a human carcinogen [18], it is used as a chemotherapy drug administered for treating

✉ Juliana M. Juárez
jjuarez@frc.utn.edu.ar

[1] Centro de Investigación en Nanociencia y Nanotecnología (NANOTEC), Facultad Regional Córdoba, Universidad Tecnológica Nacional, Maestro López y Cruz Roja Argentina, 5016 Córdoba, Argentina

some types of cancer. It is mainly used to treat chronic lymphocytic leukemia, low-grade non-Hodgkin's lymphoma, Hodgkin's lymphoma and ovarian cancer. Chemically, it is 4-[4-bis(2-chloroethyl) amino phenyl butyric acid. It has a nitrogen mustard moiety ($ClCH_2CH_2$)2 N-, which attaches to the p-position of the benzene nucleus of 4-phenyl butyric acid and L-phenylanine. The new nanotechnologies reduce the threat to the individual and increases the likelihood of surgical outcomes, especially in anticancer treatment drugs. Chlorambucil can be included in a sphere ≅ 1.85 nm diameter, the radius of maximum approximation (see Results and Discussion section). Thus, the critical molecular size is considered to possess ≅ 1.9 nm [19, 20]. Non-all drug transporters, in addition to biocompatibility and biodegradability, also meet requirements of a physicochemical type, such as a high drug loading capacity to reduce the dose, high diffusivity, both in incorporation and release (steric hindrance), absence of modification of the drug's own sites by interaction with the transporters, and exclusion of secondary reactions of the transporter, either adverse reactions or undesired cellular interactions. MCFs (mesostructured siliceous cellular foams) are being considered for achievable pharmacological applications [4, 21]. Because surface area and uniform large pores can load the active drug, particle size distribution to regulate drug loading and release, simply functionalized surface and noble biocompatibility, these create them ideal for drug delivery systems [4, 22, 23]. MCF materials are a novel auspicious host for drug delivery systems because of their low toxicity, in vivo biodegradability, and high biocompatibility [4]. Our previous studies showed auspicious results for drugs-controlled release using the novel MCF material in KETO release, which makes it highly applicable to the treatment of diseases that need a rapid response [4]. MCFs that can be derived after the inclusion of a bulking medium in the synthesis procedure of SBA-15 [4], are composed of spherically uniform cells 15–50 nm diameter [24], exhibit high surface areas and porosities, and have adjustable pore size distributions [24, 25]. This pore size can be adjusted by varying the quantity of organic swelling agent and aging temperature. MCFs have well-defined ultralong mesopores and hydrothermally cohesive structures. MCF materials closely resemble aerogels but have unique characteristics of enhanced synthesis a long with a well-defined pore and wall structure, thick walls and elevated hydrothermal resistance [4, 25]. Their high surface areas are enclosed in cage-like mesopores up to 50 nm in diameter, interconnected by windows with diameters up to 20 nm to provide a three-dimensional continual pore system, sufficiently large to conveniently accommodate even more voluminous molecules [26]. The open large pore system gives MCF unique advantages as catalyst supports and separation media for processes involving large molecules. In addition to their specific physicochemical properties, they possess high biocompatibility and low adverse effects, which with their biodegradability, making them attractive for controlled drug release applications.

The importance of this work lies in the inclusion of Chlorambucil in a biocompatible host, such as the siliceous nanomaterial MCF (Mesostructured cellular foam), which is a potential new host for drug delivery systems, nevertheless, safety of chronic exposed patients and the long-term toxicological profiling of various modes of dosing, are steps that need to be addressed in order to be able to use silica nanoparticles in clinical trials, Kazemzadeh et al., and references therein [27]. MCF not only have excellent controlled release of CLB, but also high capacity to transport the drug, absence of chemical interactions with the drug, high pore size/critical molecular size ratio of Chlorambucil (≅ 10/1), which facilitates its diffusivity, making it a proposal nanotechnology, which is suitable for performing selective chemotherapies targeting cancer cells, compared to conventional anticancer therapies, in which cancer elimination is incomplete, with the destruction of normal cells.

2 Materials and methods

2.1 Materials

Chlorambucil ($C_{14}H_{19}C_{l2}NO_2$ Sigma-Aldrich), Tetraethylorthosilicate (TEOS, 98%, Sigma–Aldrich), Poly(ethylene glycol)-block-poly(propylene glycol)-block-poly (ethylene glycol), ($EO_{20}PO_{70}EO_{20}$, P123-Sigma–Aldrich, ≥99.0%, FLUKA), 1,3,5-Trimethylbenzene (Mesitylene, Aldrich), ammonium fluoride (NH4F, Aldrich), Buffer pH 7 (Ciccarelli) and HCl (Ciccarelli, 36–38% wt.).

2.2 Synthesis of the Mesostructured cellular foam (MCF)

For the synthesis of the MCF host, a one-pot synthesis method was used [28]. For the synthesis mesitylene, was used as a swelling agent, TEOS as the silica source, a triblock copolymer P123, as a surfactant and ammonium fluoride as a mineralizing agent. Typically, 4 g of P123 were dissolved under vigorous stirring in a solution of HCl 2 M. After complete dissolution of the surfactant 0.05 g of NH_4F and 4 mL (3.86 g) of mesitylene were added and stirred at 35 ºC for one hour. Afterwards 9.14 mL of TEOS were 9.14 ml of TEOS were added dropwise and kept under continuous stirring for 20 h at 35 ºC. Then the white mixture was placed in an autoclave and kept under static conditions for 24 h at 100 ºC. Once this time had elapsed and once at room temperature, the product was filtered and washed

with bidistilled water up to pH 7. Once the material was dry, the surfactant was removed by means of two thermal treatments. The first at 550 ºC with a ramp of 3 º/min in an inert atmosphere (N_2) at 550 ºC (ramp of 3 º/min) for 6 h and the second a calcination at the same temperature for 6 h.

The Cell diameter, and window diameter, determined according to the Frenkel-HalseyHill (FHH) theory and Broekhoff-de Boer method [29], for the ratio of TMB/P123 ≅ 0.965 w/w are 32.3 and 16.6 nm respectively, in agreeing with Lukens et al. [25]. Texture properties of both the transporter and the CLB-MCF composite are listed in Table 1.

2.3 Preparation of chlorambucil-loaded mesostructured cellular foam (MCF-CLB)

Chlorambucil-loaded Mesostructured cellular foam (MCF-CLB) was prepared by the adsorption of the drug into the porous of the MCF host in an ethanol solution. Typically, 1 g of CLB was dissolved in ethanol 50 mL at room temperature, followed by the addition of the siliceous mesoporous material MCF. The resulting mixture was kept under vigorous stirring at room temperature for 24 h. Afterward, the solid was recovered by filtration and the composite MCF-CLB was washed several times with deionized water. The amount of chlorambucil incorporated in the MCF was studied in more detail and is included as supplementary material SM1 as, "Preparation of chlorambucil-loaded Mesostructured cellular foam (MCF-CLB).

2.4 CLB Release studies

The release of the drug was implemented by simulating the physiological conditions, for which the composite was immersed, in tablet form, initially in a HCl solution (0.1 M) for two hours and then in a pH 7 buffer solution to reproduce the conditions of the organism. The experiment was performed in a bath at 37 ° C and under continuous stirring. At the specific time interval, an amount of sample was withdrawn and filtered, and the quantity of CLB was determined by UV-Vis spectrophotometry (λ = 258 nm).

2.5 Characterization

X-ray diffraction: X'Pert Pro PANalytical diffractometer, with a CuKa radiation source (k = 0.15418 nm) and X'Celerator detector based on Real Time Multiple Strip (RTMS). Diffractograms were analyzed with the X'Pert HighScore Plus software.

Textural Properties: N_2 adsorption/desorption isotherms were measured at -196 C with an ASAP 2020. The samples were degassed at 400 C. The pore size distribution was estimated using Nonlocal Density Functional Theory (NLDFT) applied for cylindrical pores of siliceous adsorbents, using the desorption branch.

Transmission electron microscopy (TEM): JEOL 2100 F with an accelerating voltage of 200 kV (point resolution of 0.19 nm) microscope.

Ultraviolet-visible diffuse reflectance spectroscopy (UV-Vis DRS): JASCO V-650 with integrating sphere for diffuse reflectance. Moreover, Thermoscientific Evolution 220 spectrophotometer was used to determine the release studies of the drug.

Fourier transform infrared spectrometer (FTIR): Nicolet Modelo iS10 has been used to characterize the vibrational spectrum of CLB and MSF.

3 Results and discussion

3.1 X-ray diffraction (XRD) and textural properties

An X-ray diffraction analysis of the support and composite was performed to determine the mesoporous structure of both materials. Figure 1 displays the low-angle XRD patterns of MCF and the MCF-CLB composite. In both samples, the pattern is well resolved and shows a strong primary peak at 2 Θ ≈ 0.4 and two weak peaks at higher angles [25]. As a result, the incorporation of CLB into the host caused no significant modifications in its mesoporous structure of MCF.

X-ray diffraction analysis is an efficient technique for determining the crystalline properties and changes in the structure of mesoporous materials. Figure 2 presents the wide-angle patterns of the host MCF, the composite MCF-CLB and the pure drug CLB. For host MCF, wide XRD peaks were observed in the range of 2θ to 20–25°, which

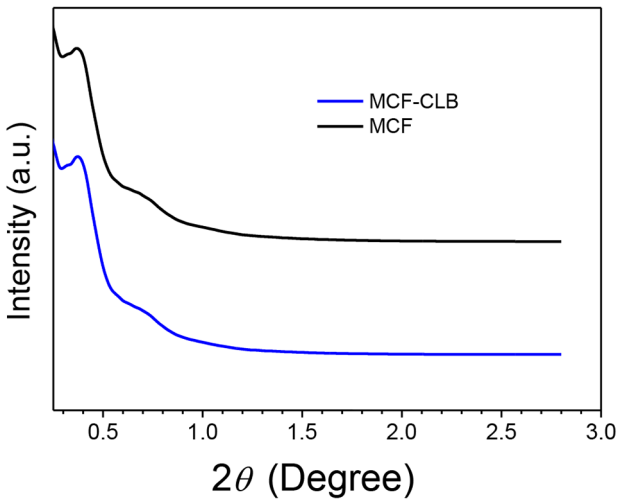

Fig. 1 Low angle XRD patterns of the host MCF and the composite MCF-CLB

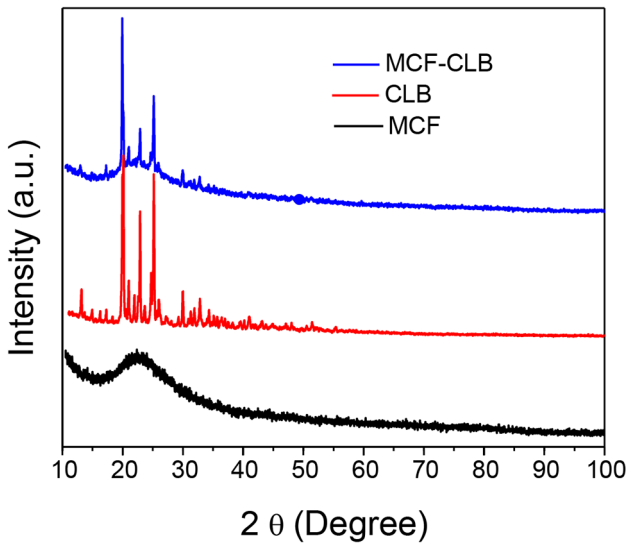

Fig. 2 Wide angle XRD patterns of MCF, MCF-CLB and pure CLB

correspond to the mesoporous nature [29]. The drug-loaded MCF XRD pattern (MCF-CLB) exhibits the characteristic peaks of CLB, indicating that the drug is present in the pores of the mesoporous foam, with its crystalline structure. However, after the adsorption of the drug, the MCF maintained the characteristic mesoporous structure.

Figure 3 shows the nitrogen adsorption-desorption isotherms at 77 K of the host and the composite. Both samples present typical IV isotherms and H1 type hysteresis loop, characteristics of mesoporous cellular foam [29]. Interestingly, both host and composite showed similar isotherm pattern and pore size distribution, which indicates that the mesostructure of the host remained after the incorporation of the drug. Table 1 presents the summarized textural properties of both samples. There is a significant reduction in surface area and pore volume for the composite MCF-CLB confirming that the drug was successfully incorporated into the pores of the mesoporous cellular foam. Both samples, host and composite, have a wide pore size distribution, with diameter averages of 17 and 15.2 respectively. For the composite MCF-CLB there is a considerable reduction in the quantity of pores with that broad distribution (Fig. 3a-b).

Considering that the CLB load in the host is 60% by weight, the results shown in Table 1, here it can be inferred that the area occupied by CLB is 76% of the total, the pore volume occupied by CLB are 64%, while the pore size decreased by only 10.58%. These results include the existence of microporosity, as shown by NLDFT MCF, with several mesopore diameters around a central mesopore, which is the most abundant (17–20 nm). When CLB is loaded, it is in the liquid phase, diffuses through the mesopores and micropores. When drying the composite for controlled release studies and textural characterization, the CLB is in a

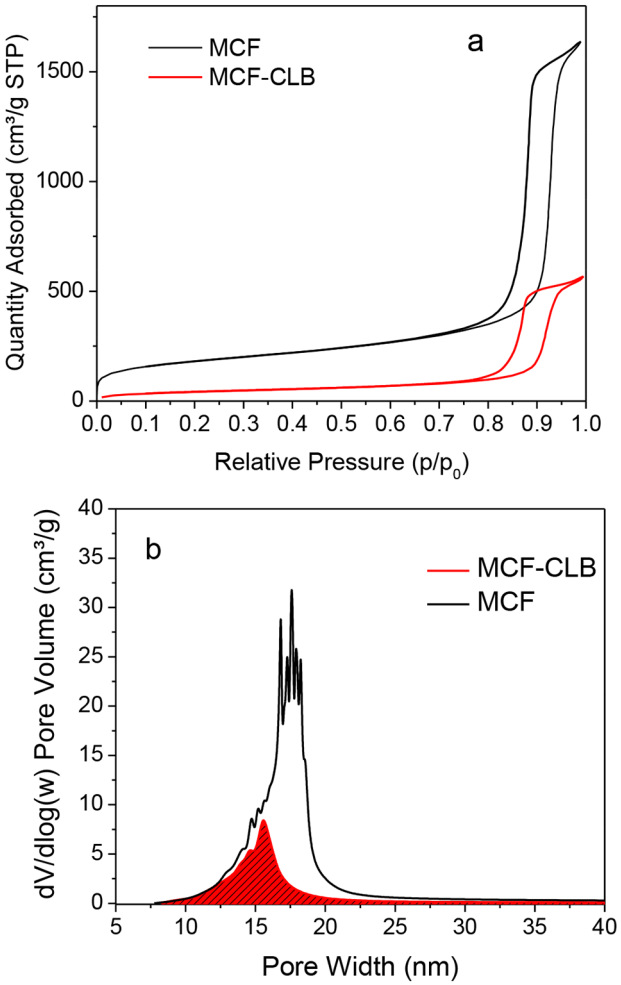

Fig. 3 N_2 adsorption-desorption isotherms (a), and pore size distribution of MCF and MCF-CLB (b)

solid state (see XRD and FTIR studies), with the possibility of blockage of micropores by crystal growth (see Sect. 3.5. Simulated 2D and 3D Optimized Structural Geometry of Chlorambucil, where it is shown that the critical molecular volume is 0.770 nm^3), which have no influence on the pore size reported in Table 1 (mesopores) but do affect the area occupied and the free volume available in the composite

3.2 TEM studies

Figure 4 provides TEM images of both, host and composite, MCF (a) and MCF-CLB (b). For the case of the host, it exhibits a well-ordered porous nature of mesoporous cellular foams. The general mesoporous structure of the MCF remained unchanged after the incorporation of CLB, indicating that this incorporation does not modify the mesoporous structure of the foam, which is in accordance with the XRD and textural properties studies.

Table 1 Textural properties

Material	Surface area (m^2/g)[a]	Total Pore Volume (cm^3/g)[b]	Meso-porous Volume (cm^3/g)[c]	Micro-pore Volume (cm^3/g)[d]	Average pore diameter (nm)[e]
MCF	641.5	2.5	2.45	0.05	17
MCF-CLB	153.8	0.9	0.9	0	15.2

[a]Specific surface measured according to the multi-point BET methodology. [b] Total pore volume. [c] Mesoporous pore volume = Total Pore Volume – Micropore Pore volume. [d] Micropore volume, calculated using t-plot method. [e] Pore size using NLDFT method

3.3 Ultraviolet-visible diffuse reflectance spectroscopy (UV-Vis DRS)

Figure 5 shows the diffuse reflectance spectrum of the host, the composite and pure drug. As expected, the host shows no absorption band. The band at 252 nm is attributable to Aromatic $\pi \rightarrow \pi^*$ Transitions. The band at 305 nm is characteristic of $\pi \rightarrow \pi^*$ transitions, from methyl- and nitrogen-substituted aromatic rings in the p-position (methyl p-toluidine) [30], which appear in the analysis of the composite. The two species that generate these electronic transitions are characteristic of CLB.

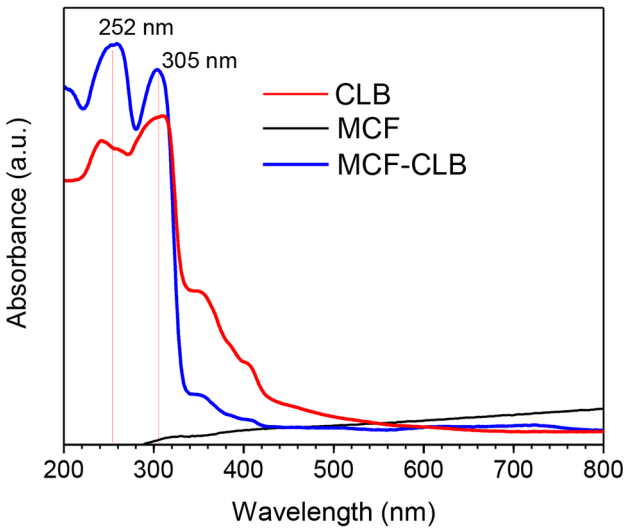

Fig. 5 Ultraviolet-visible diffuse reflectance spectroscopy of composite (MCF-CLB) and pure drug (CLB)

3.4 FTIR studies

The following study was conducted to successfully perform the vibrational analysis of chlorambucil by FTIR spectroscopy. The spectra were acquired from 4000 to 350 cm^{-1} [20, 31]. For adequate visualization of the assignment of the host (MCF) and guest (CLB) infrared absorption bands, the spectra are shown in two zones: between 4000 and 2000 cm^{-1} (Fig. 6a) and between 2000 and 550 cm^{-1} (Fig. 6b). Figure 6a, shows at 3468 cm^{-1} a weak band from the stretching of the OH bond to carbon (C-O–H) assigned to CLB, overlapped by a broad peak at 3436 cm^{-1}, corresponding to the stretching of the O-H bond attached to Si (SI-O–H), and to water molecules adsorbed on the surface of the MCF. Symmetric and asymmetric C–H stretching caused by CLB is observed at 2930 and 2977 cm^{-1} respectively.

In Fig. 6b, the bands ascribed to CLB can be assigned to the following bands: C = O stretching (1705 cm^{-1}), C-C aromatic ring (1614 cm^{-1}), C-C symmetric stretching (1570 cm^{-1}), H-C-H stretching (1520 cm-1), C = C symmetric stretching (1441 cm^{-1}), C-N asymmetric, and symmetric stretching vibrations (1341 and 1308 cm^{-1}) respectively. H–C–H bending (827 cm^{-1}), C–N–C asymmetric bending at 740 cm^{-1} and C-Cl asymmetric and symmetric stretching vibrations (562 and 545 cm^{-1}) [17]. The bands at 1080, 960, and 466 cm^{-1} are attributed to SI-O-Si, SI–OH, and Si-O stretching due to MCF.

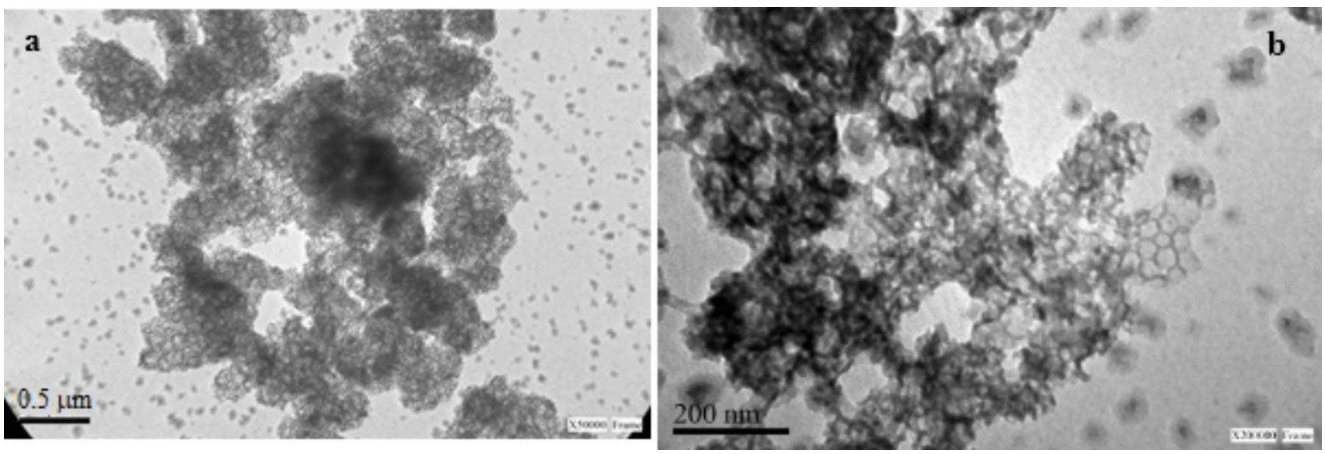

Fig. 4 TEM Images of MCF (a) and MCF-CLB (b)

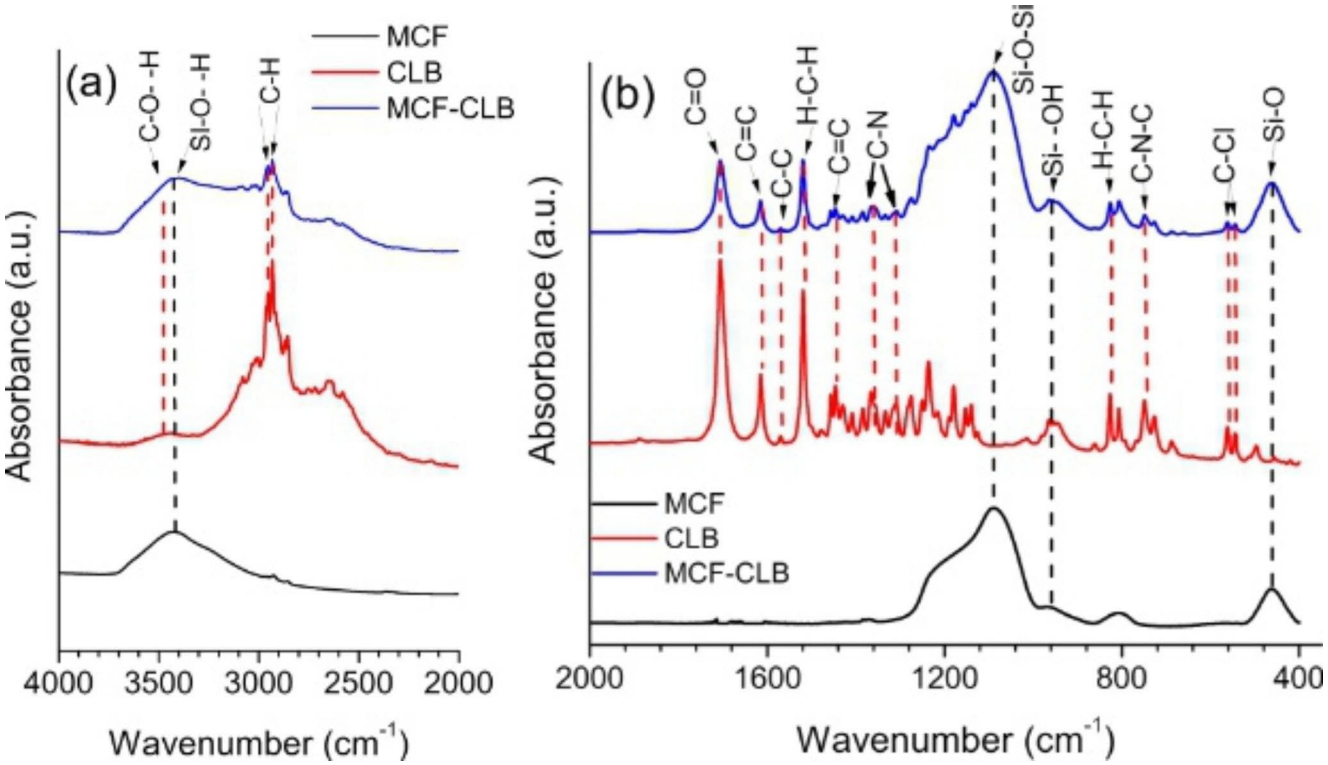

Fig. 6 Vibrational analysis of Chlorambucil by FTIR spectroscopy, (a) 4000 – 2000; (b) 2000 – 450 cm^{-1}

The appearance of the bands that characterize CLB in the MCF-CLB composite, allows us to infer that there is no chemical interaction between the guests and host so that physisorption is the predominant interaction. Additionally, the diffusion of CLB through the MCF channels and the formation of the composite is demonstrated.

The joint use of two ab initio methods, and the FTIR spectra allowed us to arrive at the most appropriate spatial

Scheme 1 CLB-MCF interaction

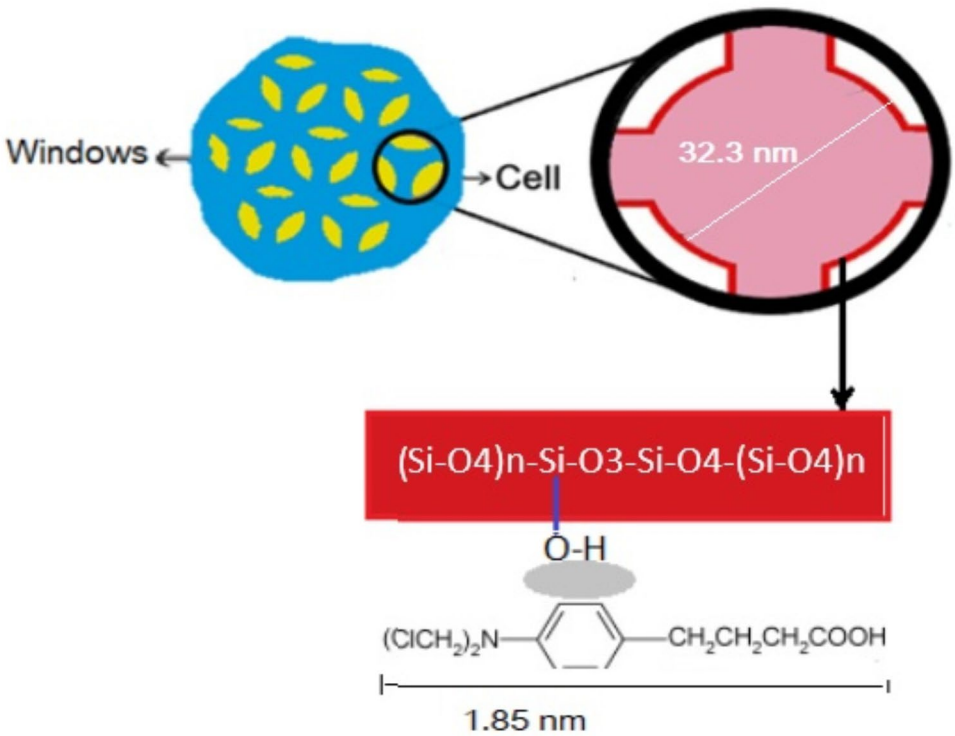

conformation of the CLB molecule (see Supplementary Material, SM2).

Scheme 1 attempts to provide a visual representation of a probable CLB model in the MCF.

Scheme 1 shows the interaction of the CLB and the polymeric silica walls of the MCF (thickness). According to Sanderson's intermediate electronegativity scale, for the (SiO4)n-SiO3–OH group, the net formal charge on the proton is only + 0.126 [32], supporting the weakness of its interaction with the π electrons of the CLB aromatic ring and the consequent reversibility.

3.5 Chlorambucil Release Studies

Drug release was realized for the first two hours in 0.1 M HCl and then in buffer pH = 7 to resemble gastric and intestinal fluid, respectively. Figure 7 shows the release of CLB contained in MCF. Dissolved commercial LEUKERAN® tablets (sugar-coated), were used as a control, releasing 80% at 2 h and entirely at 8 h (first order kinetics). While CLB release from MCF was first released rapidly (pH = 1, gastric tract) 66% at about 4 h and then continued for a prolonged time to reach 100% at 35 h, at pH 6.7 (intestinal tract), which are the absorption pathways of the drug (see Fig. 7).

The models used to fit the mechanism of chlorambucil release from the MCF matrix are the first-order kinetic model, the Schott model, the Weibull model and the Ritger and Peppas model (see Table 2). These mathematical models are widely used to determine the mechanism of drug release from a delivery system.

Korsmeyer and Peppas [33] and Ritger and Peppas [34, 35] have developed a simple, semi-empirical model, which exponentially correlates drug release with elapsed time t. In these papers they proposed their equation analyzing the drug release from a polymer matrix with Fick's law behavior and with deviation from Fick's law. The equation that describes the model is as follows:

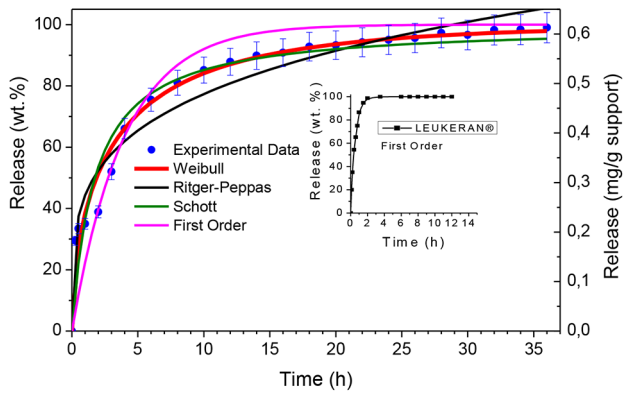

Fig. 7 Release of chlorambucil

Table 2 Fitting parameters and fitting statistics of models

	Fitting parameters	R^2	Adj-R^2	SSE	S
Ritger Peppas	k 0.443 n 0.242	0.960	0.956	0.0714	0.0613
First Order	k 0.253	0.913	0.908	0.1569	0.0864
Weibull	a 0.488 b 0.579	0.971	0.967	0.0346	0.0426
Schott	k 0.575	0.935	0.931	0.0773	0.0623

R^2 coefficient of determination, Adj-R^2 adjusted R^2, SSE final sum of squared errors, S standard deviation of the distance between the data values and the fitted values

$$\frac{M_t}{M_\infty} = \mathrm{k}t^n \tag{1}$$

where k is the constant proportional to the release rate that incorporates structural and geometrical features of the drug delivery shape and n is the release exponent, indicative of the drug-release mechanism.

However, the first-order kinetic model has been used for the absorption and elimination of some drugs and is applicable to describe the dissolution of water-soluble drugs contained in some porous matrices.

$$\frac{M_t}{M_8} = 1 - e^{-kt} \tag{2}$$

Where Mt/M∞ is the fraction of drug released at time t and k is the first-order release constant.

The Weibull function was proposed to describe the behavior of various products in which its analytical form is unknown [36]. When applied to the dissolution or release of drug from pharmaceutical dosage forms, the Weibull equation expresses the cumulative fraction released of drugs in solution Mt/M∞ at time t.

$$\frac{M_t}{M_8} = 1 - e^{-at^b} \tag{3}$$

In this equation, the scale parameter, a, characterizes the time scale of the process. The shape parameter, b, describes the curve as exponential.

The Weibull model is an empirical model. Its empirical use has been criticized [37]. The criticism focuses (i) the lack of a kinetic basis for its use and (ii) the nonphysical nature of its parameters [37]. Additionally, several attempts have been made to improve its performance [38] and validate its use [39, 40, 41].

Recently, Monte Carlo simulation techniques were used for the study of Fick diffusion of drug release in both Euclidean and fractal spaces [42,43]. It was found that the Weibull model describes very well in both cases the whole drug release curve when the mechanism of drug release

is Fick diffusion. In the case of Euclidean matrix release studied by Kosmidis et al. [42], the value of the exponent b was found to be in the range of 0.69 to 0.75. In the case of fractal release the values were found to be between 0.35 and 0.39 [43]. The Weibull function was found to arise from the creation of a concentration gradient near the Euclidean matrix release boundaries [42] or due to the "fractal kinetics" behavior associated with the fractal geometry of the environment [43].

These Monte Carlo simulation results would seemingly point to a universal law, since the Weibull model provides a simple physical connection between the model parameters and the geometry of the system.

The Schott model [44] describes second-order release kinetics and for the weight fraction of drug released would remain:

$$\frac{M_t}{M_8} = \frac{kM_8t}{1 + kM_8t} \tag{4}$$

Where k is the second order velocity constant according to the Schott model.

The unknown parameters for each model were determined by fitting the equations to the experimental data for chlorambucil release using a nonlinear least squares algorithm. Since there are differences in the number of parameters from the models, in addition to the coefficient of determination (R^2), an adjusted coefficient of determination (adjusted R^2) was incorporated into the analysis. Furthermore, the lower the value of the final SSE, the better the response is described by the model and S is an important measure of goodness-of-fit for a nonlinear model.

All statistical parameters indicate that the best model describing the phenomenon under study over the entire period is the Weibull model.

The other models describe well either the initial or final phase of the phenomenon but not in an overall mode.

The main advantage of this release is that the rate of release is fast at the beginning and then gradually decreases until 24 h practically all of the drug contained in the carrier is released (> 95%).

The value of the time exponent in the Weibull function "b" is an indicating of the transport mechanism of a drug through the polymeric matrix. Values for $b \leq 0.75$ denote Fick diffusion in Fractal or Euclidean spaces, while a combinatorial mechanism (Fick diffusion and Case II transport) is assumed to be associated with values of b in the range $0.75 < b < 1$. For values of b greater than 1, the drug transport follows a complex release mechanism. Therefore, we indicate that the material presents a Fick's law release following the Weibull model [45].

The drug release profile for CLB-MCF can be interpreted as a biphasic. Thus, there is a fast release phase associated with the diffusion of the drug, adsorbed or weakly bound, to the polymeric carrier matrix, followed by a slow release phase associated with the diffusion of the drug into the porous host or into the smaller pores.

The physisorption forces between CLB and MCF are the weak Van der Waals-type, reversible, low heat of adsorption attractive forces. Simultaneously, weak interactions are probable, as they are expected to result mainly from the interaction of the π-electrons of the aromatic ring of CLB with electron accepting sites of the MCF, such as unoccupied molecular orbitals (Lewis sites), as well as proton ceding sites such as SiOH groups. Because of the characteristic low electron delocalization capacity of the mesoporous structure, MCF structure can be assumed a weak but hard base (according to the molecular orbital theory). Thus, weak and reversible interactions between π electrons of the aromatic ring with the structural acid sites of the MCF lattice (and π-quadrupole interactions between the aromatic ring and the SiOH structural groups) would also be more likely.

Senapati et al. [46] depicted that, relying on the release kinetics (fast or sustained) of a series of LDH synthesized using co-precipitation techniques employing various anions and anticancer drugs, drug administration enhanced the in vivo course of the antitumor activity of the drug and exhibited enhanced tumor suppressive efficacy.

Consequently, as in our case (Fig. 7), the release must occur in a sustained modality, but with a fast release at the beginning (without steric hindrance between the critical molecular size of the CLB and the pore size of the host, as illustrated in the previous section, considering the 10/1 ratio of the minimum pore size of the MCF/CLB molecule), and then in a slower modality, until the complete release of the drug contained in the MCF host.

Cancerous tumors are characterized by cell division, which is no longer controlled as in normal tissues. Normal" cells stop dividing when they encounter similar cells, a mechanism known as contact inhibition. Cancer cells lose this ability. In cancer cells, the self-regulatory system that controls and limits cell division become unbalanced. The process of cell division in both normal and cancer cells is conducted through the cell cycle. This cycle goes from the resting phase, through active growth phases, to mitosis (division).

The ability of chemotherapy to destroy cancer cells depends on its ability to stop cell division. Typically, the drugs work by damaging the RNA or DNA that tells the cell how to make a copy of itself in the division [47]. If the cells cannot divide, they die. The faster the cells divide, the more probably the chemotherapy will destroy them and shrink the

tumor. Additionally, these drugs induce cell suicide (programmed cell death or apoptosis).

Chemotherapeutic drugs that destroy cells only during division are called cell cycle specific, as is the case with CLB). The timing of chemotherapy is based on the type of cell, the rate at which they divide, and the time at which a particular drug can be effective. For this reason, chemotherapy is frequently administered in cycles [52]. Thus, the rapid initial release (which is also a function of gastric pH), and subsequent prolonged release of CLB from the MCF (100% at 35 h), suggests that it is a suitable transporter to maximize its tumor activity, favoring the initial cell division (neoplastic) and facilitating contact inhibition of normal cells.

Recently S. H. Hussein-Al-Ali et al. [17] employed iron oxide nanoparticles (IONP), as CLB carriers, in which IONP acted as the nucleus and chitosan (CS, β-(1→4)-2-amino-2-deoxy-D-glucose), as the polymeric coat to construct the CLB-CS-IONP, which contains approximately 16.0 wt% CLB. The polymeric unit of the CBL-CS-IONP nanocomposite has a molecular weight of 696 g/mol, the amount of CLB carried by the nanocomposite is 0.16 mg/g, lower than the 600 mg/g of our system, with a consequent decrease in dosage. Moreover, its controlled release reached 89.9% of the drug in about 83 h (more delayed release than in this study) and was pseudo-second order regulated. Additionally, the authors studied the release at pH 7.4, ignoring the pH of the stomach (pH = 1), which is the first fluid with which it is in contact, whether it is the commercial drug or the CLB included in any transporter. Y. Zhou et al. [56] presented an article on Controlled Release of Chlorambucil in a composite of hyperbranched HPMA in the presence of β-CD. The release is like this work of an initial burst release then followed by the slower constant release, but release of CLB/MCF is faster at the beginning and slower at the end than CLB loading in HPMA- β -CD. CLB/MCF release reached practically 100% release (approx. 98%) within 30 h, which is more than enough time considering the time it takes for the body to process from the stomach to the small intestine. X. Wang et al. [57] Studied Chlorambucil loaded in mesoporous polymeric microspheres as oral sustained. Here, the release of CLB is slow and does not reach the 100% of release drug at 40 h. The best-fit model is zero-order kinetics. The advantages of using our polymeric silicates as a framework is a slow cost silicate matrix and because the release can be tailored, depending on the characteristics of silica frameworks, their textural properties and the nature of the anchoring sites.

4 Conclusions

In this study, we demonstrate an auspicious drug host material for efficient encapsulation and controlled release of CLB, performing the required therapeutic efficacy. Studies indicate that the drug is present in the pores of the mesoporous foam, without affecting the structure or chemical composition of CLB nor the mesoporous structure of the foam. The study also demonstrates that there is no chemical interaction between the guests and host so that physisorption is the predominant interaction. Additionally, the diffusion of CLB through the MCF channels and the formation of the composite is demonstrated.

The Weibull first-order kinetic model is used to fit the mechanism of chlorambucil release from the MCF matrix, the main advantage of this release is that the rate of release is fast at the beginning and then gradually decreases until 24 h practically all of the drug contained in the carrier is released (> 95%) achieved advantageous therapeutic effects.

The drug release profile for CLB-MCF can be interpreted as a biphasic, the release occurs in a sustained modality, with a fast release at the beginning, and then in a slower modality, until the complete release of the drug contained in the MCF host. Fast release can be associated with diffusion through large pores (≥ 15 nm) and slow release through smaller pores (≤ 15 nm).

Although providing a significant improvement in the controlled release of the drug and cancerous tumor treatment, chlorambucil combined nanoscale medicine should allow auspicious possible applications in effective cancer treatment.

Supplementary information The online version contains supplementary material available at https://doi.org/10.1007/s10934-022-01264-8.

Acknowledgements JMJ, JC, OAA and MGC, CONICET researchers, UTN-FRC. The authors thank FONCyT. PICT 2017–2021 1740 and PICT 2016 – 1135.

References

1. A.C. Anselmo, S. Mitragotri, J. Control Release (2014) https://doi.org/10.1016/j.jconrel.2014.03.053
2. L. Brannon-Peppas, J.O. Blanchette, AdvDrug Deliv. Rev. (2004) https://doi.org/10.1016/j.addr.2004.02.014
3. J. Cussa, J.M. Juárez, M.B.G. Costa, O.A. Anunziata, J. Mater. Sci. : Mater. Med. (2017) https://doi.org/10.1007/s10856-017-5925-4
4. J.M. Juarez, J. Cussa, M. Gomez Costa, O.A. Anunziata, Curr. Nanosci. (2018) https://doi.org/10.2174/1573413714666180222134742
5. A.G. Cheetham, P. Zhang, Y.A. Lin, L.L. Lock, H. Cui, J. Am. Chem. Soc. (2013) https://doi.org/10.1021/ja3115983
6. W. Wu, W. Driessen, X. Jiang, J. Am. Chem. Soc. (2014) https://doi.org/10.1021/ja411457r

7. J.B. Dhruba, K. Marianne, G. Mujgan, M.S. Tessa, A.M. Shaker, Int. J. Nanomed. **4**, 1–7 (2009). https://doi.org/10.2147/IJN.S4241
8. A. Roth, D.C. Drummond, F. Conrad, M.E. Hayes, D.B. Kirpotin, C.C. Benz, J.D. Marks, B. Liu, Mol. Cancer Ther. (2007) https://doi.org/10.1158/1535-7163.MCT-07-0140
9. E. Hertlein, G. Triantafillou, E.J. Sass, J.D. Hessler, X. Zhang, D. Jarjoura, D.M. Lucas, N. Muthusamy, D.M. Goldenberg, R.J. Lee, J.C. Byrd, Blood. (2010) https://doi.org/10.1182/blood-2009-11-253203
10. F. Bai, C. Wang, Q. Lu, M. Zhao, F.Q. Ban, D.H. Yu, Y.Y. Guan, X. Luan, Y.R. Liu, H.Z. Chen, C. Fang, Biomaterials. (2013) https://doi.org/10.1016/j.biomaterials.2013.04.062
11. L.Y. Chou, K. Zagorovsky, W.C. Chan, Nat. Nanotech (2014) https://doi.org/10.1038/nnano.2013.309
12. L.L. Lock, M. LaComb, K. Schwarz, A.G. Cheetham, Y.A. Lin, P. Zhang, H. Cui, Faraday Discuss. (2013) https://doi.org/10.1039/c3fd00099k
13. D. Desmaele, R. Gref, P. Couvreur, J. Control Release (2012) https://doi.org/10.1016/j.jconrel.2011.07.038
14. S. Sidipta, K.M. Arun, K. Sunil, M. Pralay, Singnal Transduct. Target. Therapy (2018) https://doi.org/10.1038/s41392-017-0004-3
15. G. Singh, B.P. Nenavathu, K. Imtiyaz, M.M.A. Rizvi, Biomed. Pharmacother. (2020) https://doi.org/10.1016/j.biopha.2020.110443
16. F. Mingliang, L. Xiaofei, L. Zonghai, W. Hongyang, Y. Danbo, S. Bizhi, Eur. J. Pharm. Sci. (2015) https://doi.org/10.1016/j.ejps.2015.08.013
17. S.H. Hussein-Al-Ali, M.Z. Hussein, S. Bullo, P. Arulselvan, Int. J. Nanomedicine. (2021) https://doi.org/10.2147/IJN.S312752
18. Report on Carcinogens, Eleventh Edition (PB2005-104914, 2004) p III-47
19. P. Huang, G. Wang, Z. Wang, C. Zhang, F. Wang, X. Cui, S. Guo, W. Huang, R. Zhang, D. Yan, Colloids Surf., B. (2020) https://doi.org/10.1016/j.colsurfb.2020.111164
20. S. Gunasekaran, S. Kumaresan, R.Arun Balaji, G. Anand, S. Seshadri, Pramana - J Phys. (2008) https://doi.org/10.1007/s12043-008-0183-0
21. S. Nanaki, M. Tseklima, Z. Terzopoulou, M. Nerantzaki, D.J. Giliopoulos, K. Triantafyllidis, M. Kostoglou, D.N. Bikiaris, Eur. J. Pharm. Biopharm. (2017) https://doi.org/10.1016/j.ejpb.2017.03.016
22. W. Xin, L. Chang, F. Na, L. Jing, H. Zhonggui, S. Jin, Mater. Sci. Eng. C (2017) https://doi.org/10.1016/j.msec.2017.04.060
23. A. Chrzanowska, A. Derylo-Marczewska, M. Wasilewska, Int. J. Mol. Sci. (2020) https://doi.org/10.3390/ijms21155479
24. L. Hermida, J. Agustian, A. Abdullah, A. Mohamed, Open. Chem. (2019) https://doi.org/10.1515/chem-2019-0107
25. P. Schmidt-Winkel, W.W. Lukens, P. Yang, D.L. Margolese, J.S. Lettow, J.Y. Ying, G.D. Stucky, Chem. Mater. (2000) https://doi.org/10.1021/cm991097v
26. R.A. Mitran, S. Ioniță, D. Lincu, D. Berger, C. Matei,. Molecules. (2021) https://doi.org/10.3390/molecules26010241
27. P. Kazemzadeh, K. Sayadi, A. Toolabi, J. Sayadi, M. Zeraati, N.P.S. Chauhan, G. Sargazi, Front. Chem. (2022) https://doi: https://doi.org/10.3389/fchem.2022.823785
28. V. Meynen, P. Cool, E.F. Vansant, Micropor. Mesopor. Mater. (2009) https://doi.org/10.1016/j.micromeso.2009.03.046
29. W.W. Lukens, P. Schmidt-Winkel, D. Zhao, J. Feng, G.D. Stucky, Langmuir. (1999) https://doi.org/10.1021/la990209u
30. K.H. Bhadra, G.D. Yadav, Microporous Mesoporous Mater. (2018) https://doi.org/10.1016/j.micromeso.2017.12.017
31. C. Sivakumar, A. Gopalan, T. Vasudevana, W. Ten-Chin, Synth. Met. (2002) https://doi.org/10.1016/S0379-6779(01)00481-7
32. S. Gunasekaran, S. Kumaresan, R. Arun Balaji, G. Anand, Asian J. Chem. **20**, 6149–6162 (2008)
33. R.T. Sanderson, J. Am. Chem. Soc. (1983) https://doi.org/10.1021/ja00346a026
34. R.W. Korsmeyer, R. Gurny, E. Doelker, P. Buri, N.A. Peppas, Int. J. Pharm. (Amsterdam, Neth.). (1983) https://doi.org/10.1016/0378-5173(83)90064-9
35. P.L. Ritger, N.A. Peppas, J. Controlled Release. (1987) https://doi.org/10.1016/0168-3659(87)90034-4
36. P.L. Ritger, N.A. Peppas, J. Controlled Release. (1987) https://doi.org/10.1016/0168-3659(87)90035-6
37. W. Weibull, J. Appl. Mech. (1951) https://doi.org/10.1115/1.4010337
38. P. Costa, J.M. Sousa Lobo, Eur. J. Pharm. Sci. (2001) https://doi.org/10.1016/S0928-0987(01)00095-1
39. T. Schreiner, U.F. Schaefer, H. Loth, J. Pharm. Sci. (2005) https://doi.org/10.1002/jps.20226
40. P. Macheras, A. Dokoumetzides, Pharm. Res. (2000) https://doi.org/10.1023/A:1007596709657
41. Z. Elkoshi, On the variability of dissolution data. Pharm. Res. **14**, 1355–1362 (1997). https://doi.org/10.1023/A:1012108402682
42. P. Lansky, M. Weiss, J. Pharm. Sci. (2003) https://doi.org/10.1002/jps.10419
43. K. Kosmidis, P. Argyrakis, P. Macheras, Pharm. Res. (2003). https://doi.org/10.1023/a:1024497920145
44. K. Kosmidis, P. Argyrakis, P. Macheras, J. Chem. Phys. (2003) https://doi.org/10.1063/1.1603731
45. H. Schott, J. Pharma Sci. (1992) https://doi.org/10.1002/jps.2600810516
46. V. Papadopoulou, K. Kosmidis, M. Vlachou, P. Macheras, Int. J. Pharm. (Amsterdam, Neth.). (2006) https://doi.org/10.1016/j.ijpharm.2005.10.044
47. S. Senapati, R. Thakur, S.P. Verma, S. Duggal, D.P. Mishra, P. Das, T. Shripathi, M. Kumar, D. Rana, P. Maiti, J. Control Release. (2016) https://doi.org/10.1016/j.jconrel.2016.01.016
48. T. Britannica, Editor of Encyclopaedia (2017, June 28). Alkylating agent. Encyclopedia Britannica. https://www.britannica.com/science/alkylating-agent
49. A. Dasgupta, C.A. Hammett-Stabler, C.R. McCudden, Therapeutic drug monitoring of antineoplastic drugs, in *Therapeutic drug monitoring data*, 3rd edn., ed. by C.A. Hammett-Stabler, A. Dasgupta (AACC Press, Washington, DC, 2007), pp. 209–220
50. A.J. Shah, C. Lenarsky, N. Kapoor, G.M. Crooks, D.B. Kohn, R. Parkman, K. Epport, K. Wilson, K. Weinberg, J. Pediatr. Hematol. Oncol. (2004) https://doi.org/10.1097/00043426-200402000-00004
51. J.H. Zao, T. Schechter, W.J. Liu, S. Gerges, A. Gassas, R.M. Egeler, E. Grunebaum, L.L. Dupuis, Biol. Blood Marrow Transplant. (2015) https://doi.org/10.1016/j.bbmt.2015.05.006
52. M. Cavo, G. Bandini, M. Benni, A. Gozzetti, S. Ronconi, G. Rosti, E. Zamagni, R.M. Lemoli, A. Bonini, A. Belardinelli, M.R. Motta, S. Rizzi, S. Tura, Bone Marrow Transplant. (1998) https://doi.org/10.1038/sj.bmt.1701280
53. I. Athanasiadou, Y.S. Angelis, E. Lyris, H. Archontaki, C. Georgakopoulos, G. Valsami, J. Pharm. Biomed. Anal. (2014) https://doi.org/10.1016/j.jpba.2013.12.004
54. H. Tesfaye, R. Branova, E. Klapkova, R. Prusa, D. Janeckova, P. Riha, P. Sedlacek, P. Keslova, J. Malis, Ann Transpl. (2014) https://doi.org/10.12659/AOT.889933
55. D. Danso, P.J. Jannetto, R. Enger, L.J. Langman, Ther. Drug Monit. (2015) https://doi.org/10.1097/FTD.0000000000000159
56. D. French, K.K. Sujishi, J.R. Long-Boyle, J.C. Ritchie, Ther. Drug Monit. (2014) https://doi.org/10.1097/01.ftd.0000443060.22620
57. Y. Zhou, Z. Guo, Y. Zhang, W. Huang, Y. Zhou, D. Yan, Macromol. Biosci. (2009) https://doi.org/10.1002/mabi.200900110

58. X. Wang, Y. Cao, H. Yan, M. Sci Eng, https://. C Mater. Biol. Appl. (2018). doi:https://doi.org/10.1016/j.msec.2018.05.078

Publisher's note Springer Nature remains neutral with regard to jurisdictional claims in published maps and institutional affiliations.